Perovskite Solar Cell Lab Course for Undergraduate Engineering Students

Angelika Basch[1,2,3], Julian Schürz[1], Verena Hartinger[1], Raimund Haslehner[1], Verena Kaltenberger[1], Sandra Mitterhuber[1], Erik Stuppacher[1] and Luca Benedek[1]
[1]University of Applied Sciences Upper Austria, Stelzhammerstrasse 28, 4600 Wels, Austria
[2]Strömstad Academy, SE-45280 Strömstad, Sweden
[3]angelika@basch.at

Abstract

Perovskite solar cells are a recently emerged photovoltaics technology that showed an impressive gain in improvement and have reached a certified efficiency of 23.7% in 2018 for research cells. Although containing toxic materials such as lead, these solar cells are currently getting a lot of attention by researchers since they can be produced by using relatively simple wet chemistry based on abundant materials, with process temperatures limited at 500 °C. This paper presents the results of a four days (or 30h) undergraduate engineering lab course using basic equipment (without major adaptions such as inert gas techniques) on the preparation and characterization of perovskite solar cells, where third year students are trained in photovoltaics and material science, research methods and characterization techniques (such as scanning electron microscopy), project management, while gaining a deeper understanding for emerging photovoltaics technologies.

Key-words: Solar Cells, Photovoltaics, Perovskites, Higher Education, Lab Course

1. Introduction

In photovoltaics-research perovskite solar-cells are widely known as one of the major breakthroughs of the last decade. Since its beginnings in 2009 (Kojima *et al*. 2009), when power conversion efficiencies were a mere 3.8%, this value has risen to 23.7% in 2018 for research devices, a value that can compete with silicon based solar cells (NREL 2019). The big advantage of perovskite solar cells is their simplicity of production. These solar cells can be produced by using relatively simple wet chemistry, with manufacturing temperatures not exceeding 500 °C (MRS Bulletin 2015). There are some commercial start-ups that mainly focus on perovskite-silicon tandem design, but not yet in the marketplace.

Perovskite solar cells also have some disadvantages. Many of the materials used in the production process are toxic and the perovskite material is sensitive to water, which makes it highly prone to rapid degradation in moist environments and releases toxic Pb^{2+} in the environment. Unlike Cd in CdTe solar cells, this toxic ion is not bound stable in a covalent compound and solar cells decompose after a few weeks when left on air. Therefore, current research focuses on stabilising the material and finding less toxic material alternatives.

The term perovskite describes the crystal structure of a calcium titanium oxide – the mineral $CaTiO_3$ in (ABX3 structure). An often-used material in photovoltaics is $CH_3NH_3PbI_3$ with methyl-ammonium iodine (MAI, CH_3NH_3I) in A position, lead (Pb) in B and iodide (I) in X position. The crystal structure consists of an inorganic framework of BX6 octahedra with the voids occupied by A cations. Record efficiencies have been obtained by mixing different A and X ions and tuning their relative proportions such that photocurrent and photovoltage are simultaneously optimized.

Figure 1 shows the schematic of a perovskite solar cell in which the active layer consists of mesoporous TiO_2, which is hosting the perovskite absorber crystal next to a scanning electron micrograph showing the morphology of the different layers.

Similar to dye-sensitized solar cells, the perovskite material is inserted (e.g. spin-coating) onto a charge-conducting mesoporous scaffold – such as titanium dioxide TiO_2 – as light-absorber. The active layer is contacted with an n-type material for electron extraction (bottom) and a p-type material for hole extraction (top) and charge generation and extraction. After light absorption in the perovskite the photo generated

doi:10.18086/swc.2019.50.02 Available at http://proceedings.ises.org

electron is injected into the mesoporous TiO_2 through which it is extracted. The simultaneously generated hole is transferred to the p-type material (top). The photo-generated electrons are transferred from the perovskite layer to the mesoporous sensitized layer, from where they are transported to the electrode and extracted at the contactor to the connected circuit. At the backside the holes are transported to the contactor by the p conductor, which may be made of spiro-OMeTAD (a very expensive p-conducting material) or copper thiocyanate (a cheaper alternative) or graphite as in this work.

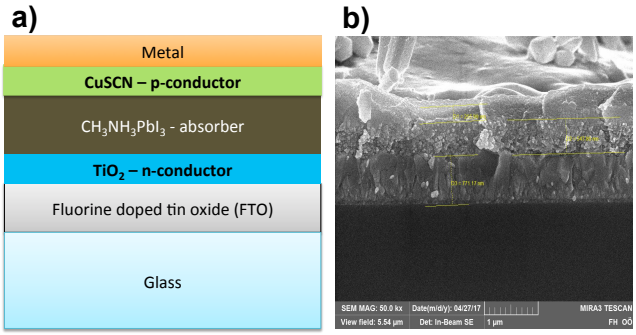

Figure 1 a) Schematic of a perovskite solar cell in a research solar cell done at Upper Austrian University of Applied Sciences. b) Scanning electron micrograph of a perovskite solar cell cross section. The SE micrograph was done with a Schottky FE-Kathodensystem field emitter (TESCAN MIRA3 LMH FE-REM with Oxford AZtec Energy EDX for element analysis). The scale bar is 1mm. (Basch Arafa 2017)

In a previous student research project we could demonstrate that it is possible to build and characterise a fully working thin an organic-inorganic perovskite hybrid solar cell in basic teaching labs without major adaptions such as inert gas techniques (Basch Arafa 2017).

This paper focuses on the manufaction of an organic-inorganic perovskite hybrid solar cell developed by 3rd year engineering students. A full day was spent at a leading research lab, the Fraunhofer Institute for Solar Energy Systems (ISE) in Freiburg to expose students to cutting edge research related to their own project where they were able to collect ideas and tips on the solar cells structure and procedure while gaining deeper knowledge about solar cell materials and their characterisation and emerging photovoltaic technologies.

2. Preparation of Perovskite Solar Cells

The perovskite material is applied in a one step method as described by Padwardhan *et al*. (Padwardhan *et al*. 2015). The porous titania layer was deposited by an in-house built low-cost spray-pyrolysis system and process, while the more dense titania layer was deposited by an in-house built low-cost spin-coater. The carbon was deposited by applying dispersed carbon in acetone by a soft brush.

Figure 2 shows the perovskite solar cell scheme based on a scaffold of porous and more-dense titania layer and graphite used in this project. The project is based on experience of previous student groups working on this topic (Hauthaler *et al*. 2018, Bamberger *et al*. 2015).

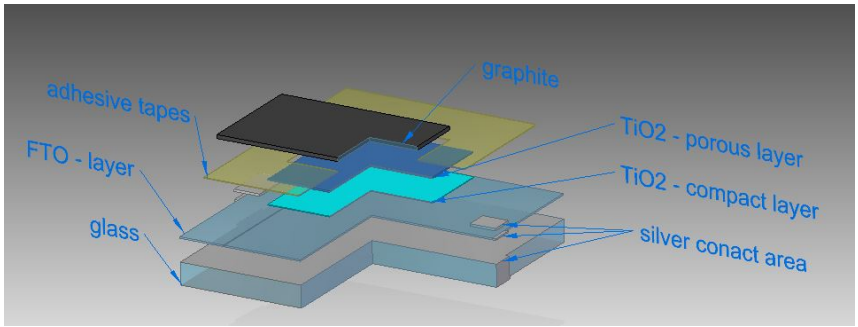

Fig. 2: Perovskite solar cell structure based on a scaffold of compact and porous TiO_2 and graphite. The size of the substrate is 3.3x3.5mm

The following steps / layers are processed in this order using glass coated FTO as a substrate

1. Deposition of compact TiO_2 layer via spray pyrolysis or spin coating

2. Deposition of porous TiO_2 layer via screen printing or spin coating

3. Deposition of ZrO_2 layer

4. Masking of the cell

5. Deposition of graphite layer

6. Applying of contacts

7. Inserting perovskite crystal

First a suitable production mount was built to prepare solar cells. The size of this production mount was limited by the muffle furnace, hence, the quantity of the cells produced on one batch was limited to eight. The production mount shown in Figure 3 was constructed in Solid Edge, a program for 3D visualization: Baseplate (1): The baseplate is an aluminium block. To produce eight solar cells a surface area of a length of 200 mm and a width of 110 mm is needed. Adjustment plate (2): The purpose of the adjustment plate is to attach the cells. As can be seen, there are always two cells in a row. Therefore, it is necessary to tight everything smooth, since it is important that the cells and other parts of the production mount are able to expand during the heating process to avoid cracking. Baseboard (3): The Baseboard is the counterpart of the adjustment plate (2). The baseboard is rigidly mounted on the baseplate. Space bar (4): To avoid contact between the cells during the manufacturing process, a space bar was inserted. Stencil (5): After all cells are aligned and prepared the required stencil will be mounted on top of the production mount. There are three different types of stencils that can be used as template for TiO_2 layer the space layer (ZrO_2) and template for the graphite layer. Each stencil was manufactured in two different thicknesses. The reason for this was the unknown influence of the high temperatures on a stencil with a thickness of 0.5 mm. The second stencil with a thickness of 0.8 mm was used as a backup system

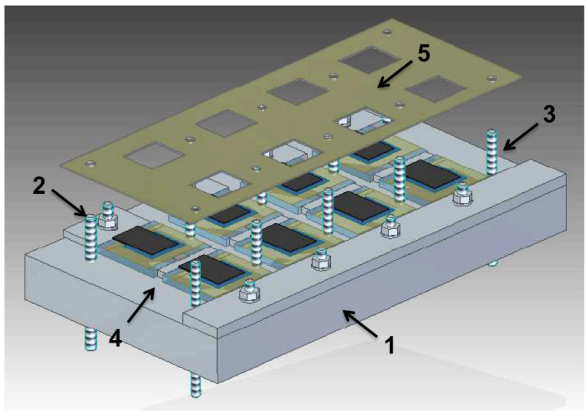

Fig. 3: The production mount was constructed by Solid Edge and the size limited by the muffle furnance to 200x110cm.

Then glass pieces measuring 3.3 x 3.5 cm were made. The glass is already coated with a transparent, conductive oxide the FTO (fluorine doped tin oxide) layer and shown in the red area in Figure 4 left. The material has a low absorption in visible light and thus does not affect the functionality of the solar cell. For contact separation, this FTO layer was scratched in a way that a short circuit is prevented at a position of the glass to make two contacts to characterise them. The contact separation was carried out in two different ways. On the one hand mechanically, with a diamond scratch and on the other hand chemically, by etching using a reaction of zinc and hydrochloric acid. This separation was set at 5 mm from the outside edge.

2.1. The compact titanium oxide layer was applied by two different methods, spray pyrolysis or spin coating

a: Deposition of compact TiO_2 by spray pyrolysis: For the application by spray pyrolysis, the cells of the first batch were fixed in the production mount (as shown in Figure 2) and then preheated to 450 °C in the muffle furnace. For the precursor solution titanium diisopropoxide bis(acetylacetonate) (Sigma Aldrich) was mixed with ethanol 1/19 and filled into a commercial airbrush gun. After the cells reached their temperature of 450°C, 10 layers of titanium oxide-ethanol mixture were applied. The cells and the production mount were

then placed back in the muffle furnace to heat up again. This process was repeated 10 times to reach a total of 100 layers. Due to the inhomogeneity of the porous TiO_2 layer as shown in Figure 4 left, which subsequently became visible in the scanning electron microscope, the mixing ratio was increased to 1/38 in the second batch and a total of 200 layers were applied. This resulted in a much more homogeneous layer as shown in Figure 4 right.

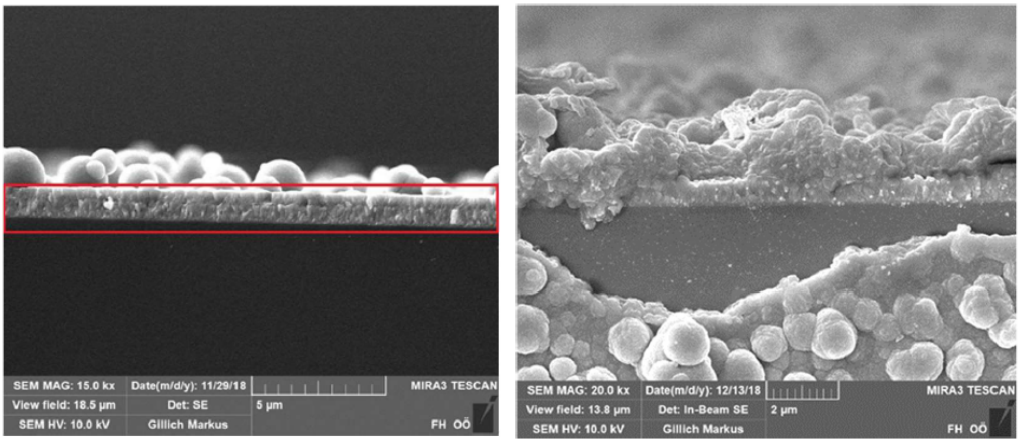

Fig. 4: Left: The red area indicates the FTO layer the spherical structure is TiO_2 deposited by spray pyrolysis by a concentration of 1/19. Right: TiO_2 deposited by spray pyrolysis in a concentration of 1/38 results in a more homogenous deposition of TiO_2. The SE micrographs were done with a Schottky FE-Kathodensystem field emitter (TESCAN MIRA3 LMH FE-REM with Oxford AZtec Energy EDX for element analysis). The scale bar is 5µm on the left and 2µm on the right.

b: Deposition of compact TiO_2 via spin coating

To deposit compact TiO_2 via the spin coating method one cell was subsequently mounted in the spin coater (as illustrated in Figure 5 right) and the TiO_2 precursor solution described in 2.1.a was added with a pipette. The spin coater was set to 2000 rpm and each cell was spin-coated for 60 seconds at full speed. The adhesive tape was then removed, and the cells were placed in the muffle furnace at 475 °C for 30 minutes. As can be seen in Figure 5 left, a very thin and homogeneous TiO_2 layer was produced using this method.

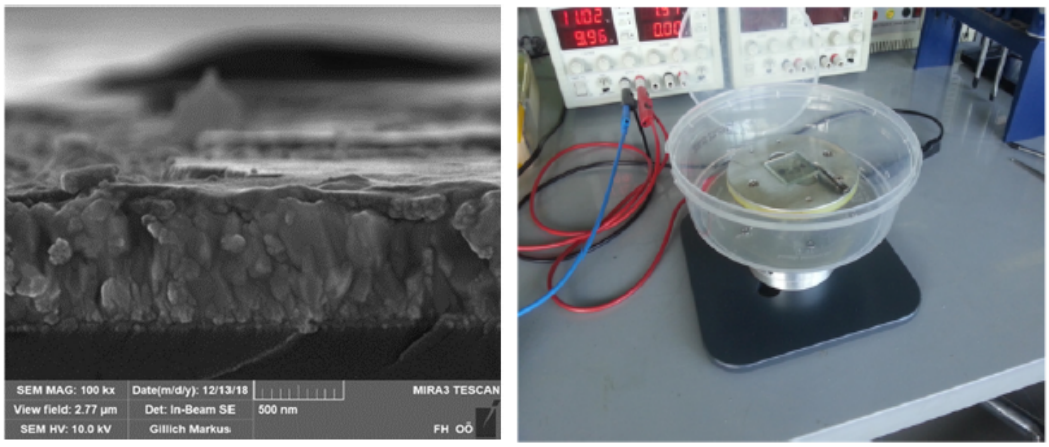

Fig. 5: Left: compact TiO_2 deposited via spin coating. The SE micrograph was done with a Schottky FE-Kathodensystem field emitter (TESCAN MIRA3 LMH FE-REM with Oxford AZtec Energy EDX for element analysis). The scale bar is 500nm. Right: In-lab built spin coater.

2.2 The porous titanium oxide layer was applied by two different methods, screen-printing or spin-coating

The porous TiO_2 layer should later be able host the perovskite crystals. Again, two different application methods were used.

a: Deposition of porous TiO_2 via screen printing process

To be able to apply TiO_2 with the screen-printing method, the desired area must first be masked. The TiO_2

paste is then applied to one side of the cell with a spatula. Now the adhesive tape is removed again, and the layer is pre-dried with a hot air dryer (Figure 6 right). In the last step, the cells are annealed at 500 °C for approximately 15 minutes in the muffle furnace. Under the electron microscope the layer applied in this way is relatively thick but homogeneous (Figure 6 left).

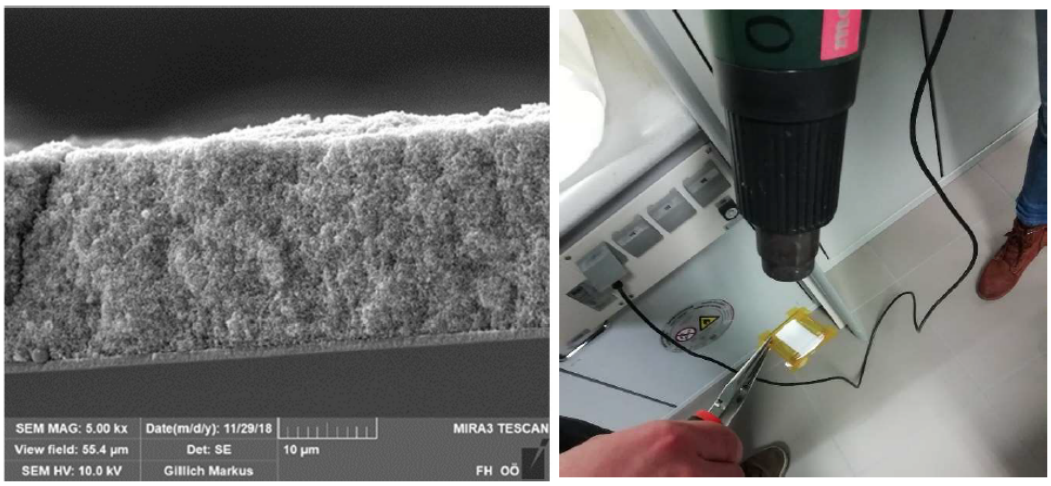

Fig. 6: Left: Deposition of porous TiO_2 via screen printing. The SE micrograph was done with a Schottky FE-Kathodensystem field emitter (TESCAN MIRA3 LMH FE-REM with Oxford AZtec Energy EDX for element analysis). The scale bar is 10µm. Right: Sample of TiO_2 coated FTO glass dried by hot air dryer.

b: Deposition of porous TiO_2 by spin coater

In order to apply the porous TiO_2 layer with the spin-coating process, the desired area must be masked again. The cell is then fixed in the spin coater and the TiO_2 solution is dripped on with a pipette. Now the cell is spin-coated with 2000 revolutions per second for 60 seconds. At the end of the process, the adhesive tape is removed again, and the cells are annealed at 550 °C for 60 minutes. Under the electron microscope it can be seen (Figure 7) that the layer applied in this way is very thin and homogeneous.

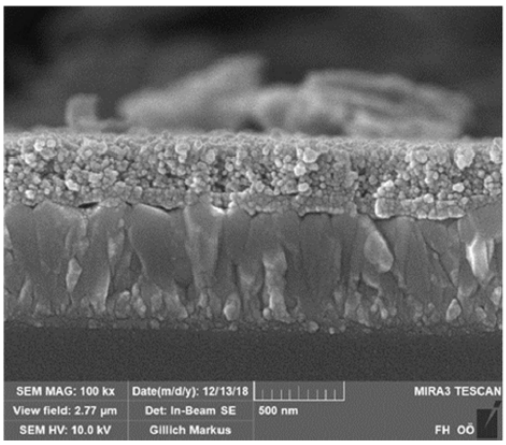

Fig. 7: Porous TiO_2 via spin coating. The SE micrograph was done with a Schottky FE-Kathodensystem field emitter (TESCAN MIRA3 LMH FE-REM with Oxford AZtec Energy EDX for element analysis). The scale bar is 500nm.

2.3. Deposition of ZrO_2

The zirconium dioxide (ZrO_2) layer is deposited between the porous titanium dioxide (TiO_2) layer and the graphite back contact, thereby direct contact is avoided. It serves as a hole transportation layer (HTL), and thereby increases the selectivity of the graphite back contact. As recombination is reduced the open circuit voltage is higher (Tress *et al*. 2014).

The used ZrO_2 was in a powder form (SigmaAldrich). To be able to create a consistent, even layer a paste has been created. The use of ethanol as a solvent proved to have the best results.

Experiments were done with two heterogeneous mixtures of the 20 and, respectively 40 mg, ZrO_2 powder in 4ml ethanol. To apply the mixture to the cell, the edge was covered by a simple tape (no need for heat resistant tape). The cell was fixed into the spin coater and 0.16 ml of the mixture was dropped on the surface. The cell was rotated at 3250 rpm for 30 seconds.

The ZrO_2 layer was not visible in SEM. The two cells produced in the same batch, one with HTL and one without HTL, were measured under the same conditions. No relevant advantage of the HTL could be seen in the open circuit voltage (V_{OC}) or the short circuit current (I_{SC}), however the cell with HTL has a slightly better fill factor. Hence, it is recommended to use slower rotation speeds in the spin coater and higher concentration of ZrO_2 on the cell.

2.4. Masking of the cell

For the masking three different tapes were used: Tesa Painter's Crepe Paper Tape, regular adhesive office tape (Tixo) and a heat resistant (Capton) tape. The main aim of the tape is to serve as a barrier for fluids, which are to be deposited onto the cells. The type of tape depends mainly of the type of the fluid and the temperature necessary for following processes. Note: Not only the current, but also the following process temperatures should be kept in mind.

2.5. Deposition of the graphite layer

The graphite layer as the back electrode collects the holes and is positioned between the silver contacts and the HTL or perovskite. For the cells 95-98 % graphite (electrically conductive material mainly used in Li-ion batteries) was used. To obtain a constant thickness of the layer dry graphite was mixed with acetone in the ratio of about 8:100 (for eight cells an amount of 0.15 g graphite mixed with 2 ml of acetone). A short time in an ultrasonic bath is recommended to make sure the graphite particles don't coagulate. The mixture can simply be applied using a soft brush, shortly after the ethanol is deposited it evaporates and a thin graphite layer is formed, as it can be seen in Figure 8 as scanning electron micrograph left and a photo right.

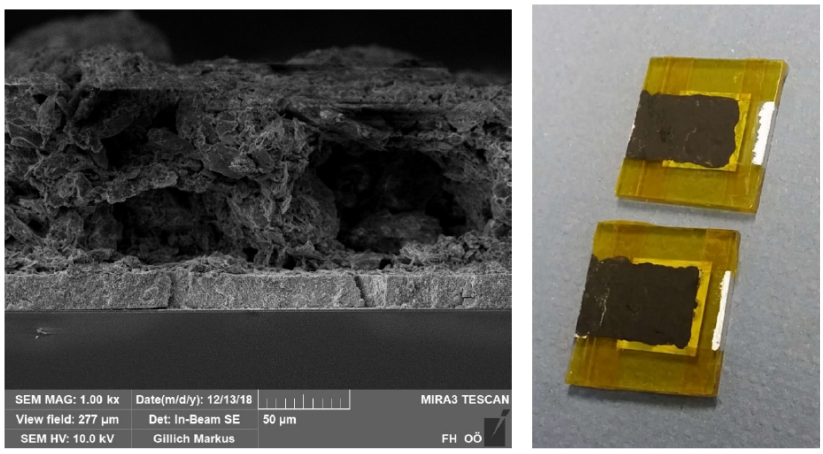

Fig. 8: Left: Scanning electron micrograph of graphite layer The SE micrograph was done with a Schottky FE-Kathodensystem field emitter (TESCAN MIRA3 LMH FE-REM with Oxford AZtec Energy EDX for element analysis). The scale bar is 50µm. Right: Finished cells with silver contacts and heat resistant Capton tape.

2.6. Applying of contacts

For measuring the cells two contact points are needed. One contact point at each side of the substrate on top of the FTO layer. The contacts where realized with commercial silver paste. This paste can easily be brushed on the sides and on top of the glass.

2.7. Inserting perovskite crystal

The last step of the production of the cells applying in the perovskite. A perovskite precursor ink (Ossila) preheated for two hours with 70 °C and 36 µl was dripped onto the graphite layer. This solution contains Pb^{2+}-ions. Take suitable precautions. This ink sinks into the cell and forms under heat influence and in combination with the TiO_2 a crystal structure.

3. Characterisation of Perovskite Solar Cells

3.1 Measurement setup

The light source used to measure the cells was a small test stand equipped with three halogen lamps of 150W each at a maximum of 17 V DC, in order to generate an irradiance of 1000 W/m². The halogen lamps are controlled by a power supply unit where the voltage and thus also the illuminance of the lamps can be regulated. The entire measurement setup including the measuring devices used is shown in Figure 9 left. To determine the irradiance on the cells, a calibrated and temperature-compensated silicon cell was placed under the test stand before each cell was measured in order to maintain the intensity at approx. 1000 W/m². The sensor used has the designation Si-01TC-batt.

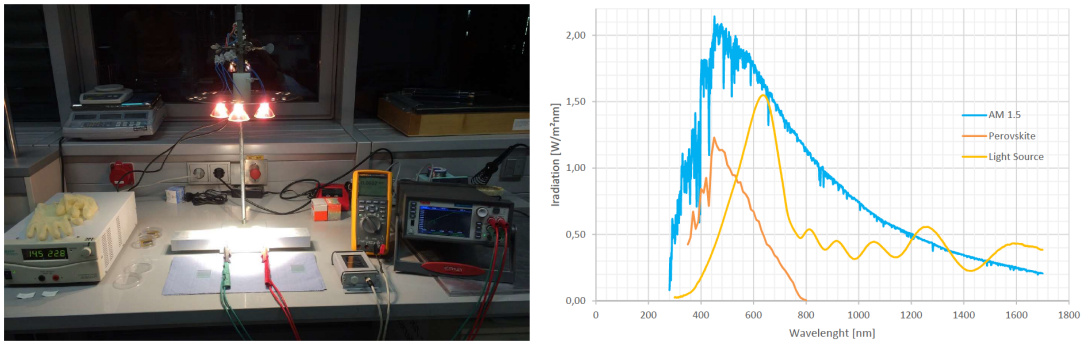

Fig. 9: Left: In house built measurement setup. Right: Spectral Mismatch, Radiation Spectrum of halogen lamp and cell performance under AM 1.5 irradiation (Bamberger et al 2015).

The spectral mismatch it will not be discussed in more detail here, but has of course an impact on the characterisation results. However, it should be pointed out again that the deviations of the halogen lamps from the AM 1.5 spectrum and thus also from the working range of the perovskite cells lead to losses in the efficiency of the cells, as only part of the spectrum of perovskite cells can be covered by the existing halogen lamps. This behaviour is illustrated again in Figure 9 right.

In order to achieve a better contacting of the front and rear contact of the cells and thus a lower contact resistance during the measurement, an additional small holder was built. This is equipped with two spring-loaded contact pins per contact and at the same time this offers a stable hold for the cell during the measuring process and shown in Figure 10.

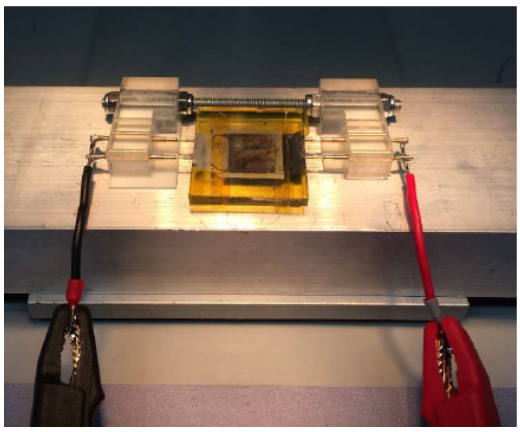

Fig. 10: In-house built solar-cell measurement system

3.2 Measuring instruments

A standard Fluke 287 True RMS multi-meter was used for the first measurements on the cells to determine the short-circuit current I_{SC} and the short-circuit voltage U_{OC}. This multi-meter provided a good accuracy

class for the first measurements in order to estimate the voltages and currents produced by the first cells. For a more detailed measurement of the cells, the Keithley 2450 SourceMeter was used. This instrument offers a much higher accuracy class and has a four-wire measurement capability that eliminates the impedances of the test leads and the measurement inaccuracies they cause. This made it possible to measure almost directly at the contact points of the cells. In addition, the measuring device has a very high accuracy class for the voltage range up to µV, as well as for the current range up to pA. This is particularly important for current measurement, as the cells produce good voltages but only very low currents, which can easily lead to measurement inaccuracies. In addition to determining I_{SC} and U_{OC}, the Keithley 2450 SourceMeter also recorded and evaluated the voltage to current characteristic.

The best resulting perovskite solar cells (about $2cm^2$) had a voltage of up to 550mV and low currents, resulting in a conversion efficiency of about 0.03% and a fill factor of about 0.5.

4. Recommendations and Outlook

Considerations on lead in perovskite

The company Ossila sells ready made precursor solutions. However, the material contains lead, which is toxic. Take suitable precautions that are in line with your organisations safety procedures!

Lead is toxic, but PV modules are currently not part of the Ordinance on the Avoidance of Lead in the Production of Electronic Equipment (RoHS). The toxicity impact during module fabrication has been denoted negligible in life cycle study (Ibn-Mohammed *et al*. 2017). Notwithstanding the above, lead-containing materials show much higher efficiencies when used as part of photovoltaic cells. Current research efforts focus on the substitution of lead with other elements such as tin (which is toxic too in its ionic form!), but these lead-free perovskite cells have only reached efficiencies of about 6% so far (Babayigit *et al*. 2015).

Cost and CO_2 emission factor of perovskite solar cells

The CO_2 emission factor for perovskite solar cells is expected to be 5g $CO_{2\ eq}$/kWh $_{el}$ in the future compared to 40g $CO_{2\ eq}$/kWh $_{el}$ for c-Si and 75g $CO_{2\ eq}$/kWh $_{el}$ for mono-Si. The cost of perovskite modules is estimated to be 75% less than conventional silicon solar cells.

Perovskite Silicon Tandems

Recently, efficiencies up to 25% have been reported for solar cells based on crystalline silicon. The theoretical limit for a single junction solar cell based on silicon (band gap of 1.1eV) - the Shockley-Queisser limit - is about 29% (Shockley Queisser 1961). As a result most of the incident solar radiation is lost and cannot be utilised for energy conversion. Solar cells with multiple thin layers made of materials with different (higher) band gaps (such as organic-inoragnic perovskite hybrids) can outperform this limit, when stacked on top of a high efficiency silicon solar cell.

3. Acknowledgements

This work would not have been possible without the financial and personal support of Michael Steinbatz, Helmut Hüttmansberger, Georg Huber and Markus Gillich from the University of Applied Sciences Upper Austria and useful discussions with Simone Mastrianni and Gayathri Mathiazhagan from the Fraunhofer Institute for Solar Energy Systems (ISE) in Freiburg.

4. References

Kojima, A. *et al*. 2009. J. Am. Chem. Soc. 131, 6050–6051.
NREL. Best Research-Cell Efficiencies (NREL, accessed 02 January 2019); https://www.nrel.gov/pv/assets/pdfs/pv-efficiency-chart.20181221.pdf
MRS Bulletin August 2015.
Basch A., Arafa S., 2017. Higher Education and Education of the Public in Energy Conversion in Austria and Egypt Photovoltaics and Electrochemical Storage. 12th International Symposium on Renewable Energy Education Proceedings ISREE 2017, 19th - 21st June in Strömstad Sweden 2017.

Hauthaler, M., Lehner, G., Pamminger, M., & Rizk, K., 2018. Perovskite Solar Cells - Project Report - Theory on Perovskite Solar Cells. Wels. Unpublished work.
Bamberger, F., Breitwieser, S., Buchegger, C., Diermaier, F., Mayr, F., Sonnleitner, C., Steinlechner, S., 2015. Organic – Inorganic Perovskite Hybrid Solar Cells. Wels: Project Report of the 4th Semester Interdisciplinary Project in the degree program Sustainable Energy Systems at University of Applied Science Upper Austria. Unpublished Work.
Padwardhan, S., 2015. Introducing Perovskite Solar Cells to Undergraduates. J. Phys. Chem. Lett. 6 (2), 251–255. DOI: 10.1021/jz502648y
Tress, W., Marinova, N., Inganäs, O., Nazeeruddin, M. K., Zakeeruddin, S. M., and Graetzel, M., 2014. The role of the hole-transport layer in perovskite solar cells - reducing recombination andincreasing absorption. IEEE. Denver, CO, USA: https://ieeexplore.ieee.org/document/6925216/citations?tabFilter=papers#citations.
Ibn-Mohammed T., Koh S. C. L., Reaney I.M., Acquaye A., Schileo G., Mustapha K.B., Greenough R., 2017. Perovskite Solar Cells: An Integrated Hybrid Lifecycle Assessment and Review in Comparison with Other Photovoltaic Technologies. Renew. Sustain. Energy Rev., 80, 1321–1344. https://doi.org/10.1016/j.rser.2017.05.095.
Babayigit A., Thanh D.D., Ethirajan A., Manca J. , Muller M., Boyen H.-G.and Conings B. 2015. Assessing the toxicity of Pb- and Sn-based perovskite solar cells in model organism Danio rerio Scientific Reports | 6:18721 | DOI: 10.1038/srep18721
Queisser H.J., Shockley W., Detailed Balance Limit of Efficiency of p-n Junction Solar Cells. Journal of Applied Physics, 1961. 32(3): p. 510.